TECHNICAL UNIVERSITY OF CLUJ-NAPOCA

ACTA TECHNICA NAPOCENSIS

Series: Applied Mathematics, Mechanics, and Engineering
Vol. 60, Issue IV, November, 2017

SYNTHESIS OF THE CAM AND DETERMINATION OF THE REDUCED ANGULAR VELOCITY AND ACCELERATION OF THE LEVER OF A DISTRIBUTION MECHANISM FOR A MILLER – ATKINSON CYCLE

Ionuț DRAGOMIR, Bogdan MĂNESCU, Nicolae-Doru STĂNESCU, Nicolae PANDREA

Abstract: *In this paper we consider a distribution mechanism used for the Miller – Atkinson cycle of an engine. The synthesis of the cam is obtained by numerical methods and geometrical considerations. Two laws of motion are used for the displacement of the valve. The reduced angular velocity and acceleration are calculated for each case. The head of the valve is considered to be spherical and planar. We also study the influence of different parameters on the reduced angular velocity and acceleration of the lever.*
Key words: *Miller – Atkinson cycle, distribution mechanism, synthesis, reduced angular velocity and acceleration, influence of parameters.*

1. INTRODUCTION

The engines which work after the Miller cycle lead to the diminishing of the NOx reduction [1], depending on the angle of the late intake valve closing. Moreover, the Miller cycle increases the efficiency based on longer expansion ratio [2]. The performances of a standard Atkinson engine can be also analyzed with the aid of the finite-time thermodynamics [3]. Early Inlet Valve Closure is used for Ford engine [4]. Late Inlet Valve Closure and Early Inlet Valve Closure lead to the reduction of soot [5] and NOx [6]. Complex theoretical and experimental study using a 3 cylinder engine in which 2 cylinders realize 4 strokes cycles, while the third one performs a 5 stroke cycle is performed in [7]. Other authors [8] consider a turbocharged Dual cycle model and, using Matlab simulation, they study the effects of different parameters. The general synthesis of a distribution mechanism with general contact curve is described in [9]. The vibrations of the engine considering different types of non-linear suspensions are discussed in [10], [11]. Aspects concerning the distribution mechanism for the Miller – Atkinson are discussed by the authors in [12, 13].

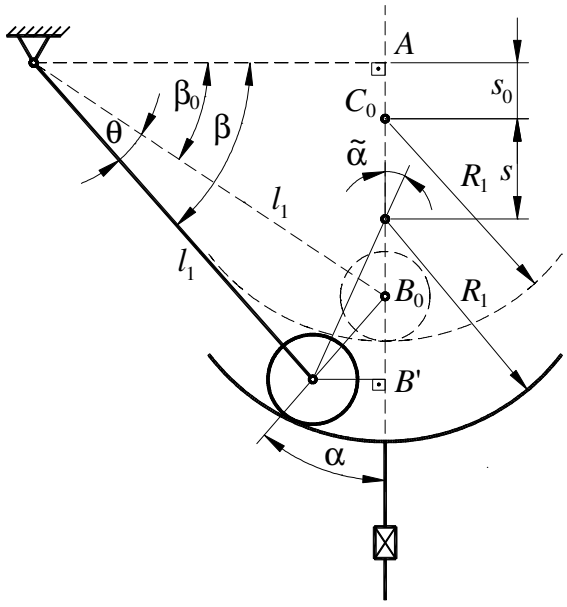

Fig. 1. Geometrical approach of the mechanism.

2. THE MECHANISM

At a displacement s of the valve, the lever rotates with the angle θ (Fig. 1).

Let B' be the projection of the point B onto the direction of the displacement of the valve and let us denote by α, and $\tilde{\alpha}$ the angles formed by the segments BB_0, and BC, respectively, with the direction of the valve's displacement.

From the relations

$$AB_0 = l_1 \sin\beta_0, AB_0 = s_0 + R_1 - R_2 \quad (1)$$

it results

$$s_0 = l_1 \sin\beta_0 - (R_1 - R_2). \quad (2)$$

We also have

$$\alpha = \beta_0 + \frac{\theta}{2}, \beta = \beta_0 + \theta, \quad (3)$$

$$BB_0 = 2l_1 \sin\frac{\theta}{2}, \quad (4)$$

$$\sin\tilde{\alpha} = \frac{l_1[\cos\beta_0 - \cos(\beta_0 + \theta)]}{R_1 - R_2}, \quad (5)$$

$$\tilde{\alpha} = \arcsin\left(\frac{l_1[\cos\beta_0 - \cos(\beta_0 + \theta)]}{R_1 - R_2}\right), \quad (6)$$

$$\begin{aligned} AB' &= s_0 + s + (R_1 - R_2)\cos\tilde{\alpha} \\ &= s_0 + R_1 - R_2 + B_0B' \end{aligned}, \quad (7)$$

$$\begin{aligned} B_0B' &= 2l_1 \sin\frac{\theta}{2}\cos\alpha \\ &= l_1[\sin(\theta + \beta_0) - \sin\beta_0] \end{aligned} \quad (8)$$

and one obtains the relation

$$\begin{aligned} &-s + l_1[\sin(\theta + \beta_0) - \sin\beta_0] \\ &+ (R_1 - R_2)(1 - \cos\tilde{\alpha}) = 0. \end{aligned} \quad (9)$$

From the last equation one deduces the angle θ of the lever's rotation.

The determination is performed with the aid of the Newton method. To be out to realize this thing we denote by $f(\theta)$ the function

$$\begin{aligned} f(\theta) &= -s + l_1[\sin(\theta + \beta_0) - \sin\beta_0] \\ &+ (R_1 - R_2)(1 - \cos\tilde{\alpha}), \end{aligned} \quad (10)$$

in which $\tilde{\alpha}$ is given by expression (6).

It successively results

$$\frac{d\tilde{\alpha}}{d\theta} = \frac{l_1 \sin(\beta_0 + \theta)}{(R_1 - R_2)\cos\tilde{\alpha}}, \quad (11)$$

$$\begin{aligned} f'(\theta) &= \frac{df(\theta)}{d\theta} = l_1 \cos(\theta + \beta_0) \\ &+ l_1 \operatorname{tg}\tilde{\alpha} \sin(\beta_0 + \theta) \\ &= \frac{l_1}{\cos\tilde{\alpha}} \sin(\theta + \beta_0 + \tilde{\alpha}), \end{aligned}, \quad (12)$$

$$\Delta\theta = -\frac{f(\theta)}{f'(\theta)}, \quad (13)$$

the actualization being

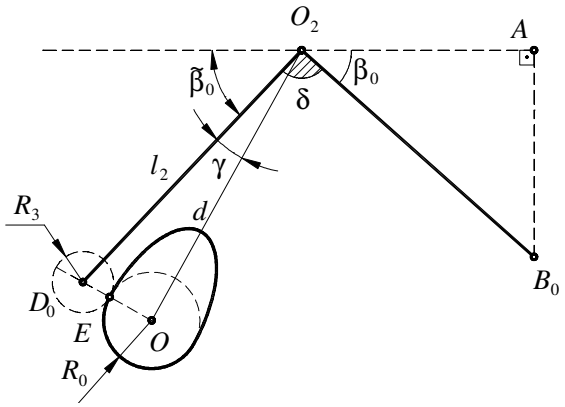

Fig. 2. The repose position

$$\theta \mapsto \theta + \Delta\theta. \quad (14)$$

One cycles the procedure until

$$|\Delta\theta| < \varepsilon, \quad (15)$$

where the error ε has the expression

$$\varepsilon = 0{,}001°. \quad (16)$$

As initial value for the angle θ one considers the value of θ from the previous step.

3. THE SYNTHESIS OF CAM

3.1. The repose position

From Fig. 2 we have the geometric relations

$$\tilde{\beta}_0 = \pi - \beta_0 - \delta_0, \quad (17)$$

$$\gamma = \arccos\left(\frac{l_2^2 + d^2 - (R_0 + R_3)^2}{2l_2 d}\right). \quad (18)$$

Moreover, the position of the segment OO_2 relative to the straight line perpendicular to the direction of displacement of the valve is given by the angle $\tilde{\beta}_0 + \gamma$.

3.2. The current position

The parametric equations of the roll are (Fig. 3)

$$x_2 = -l_2 - R_3 \sin\lambda, y_2 = -R_3 \cos\lambda, \quad (19)$$

where λ is a real parameter.

The contact point between the roll and the cam, denoted by E, has the coordinates:

– X_E, Y_E relative to the fixed reference system OXY;

– x_1, y_1 in the Ox_1y_1 reference system rigidly linked to the cam;

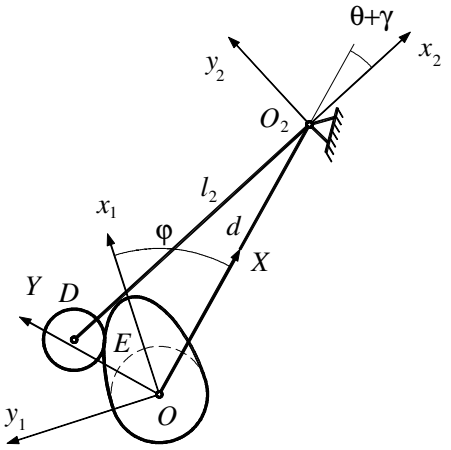

Fig. 3. The current position

– x_2, y_2 in the $O_2x_2y_2$ reference system rigidly linked to the lever.

If we denote by φ the rotation angle of the cam and by θ the rotation angle of the lever, then we have

$$\begin{aligned} X_E &= x_1\cos\varphi - y_1\cos\varphi = d \\ &+ x_2\cos(\theta+\gamma) + y_2\sin(\theta+\gamma), \\ Y_E &= x_1\sin\varphi + y_1\cos\varphi \\ &= -x_2\sin(\theta+\gamma) + y_2\cos(\theta+\gamma). \end{aligned} \tag{20}$$

Multiplying the first relation (20) by $-\sin\varphi$, the second relation (20) by $\cos\varphi$ and summing the results, one successively obtains

$$\begin{aligned} y_1\sin^2\varphi + y_1\cos^2\varphi &= -d\sin\varphi \\ &- x_2\cos(\theta+\gamma)\sin\varphi \\ &- y_2\sin(\theta+\lambda)\sin\varphi \\ &- x_2\sin(\theta+\gamma)\cos\varphi \\ &+ y_2\cos(\theta+\gamma)\cos\varphi, \end{aligned} \tag{21}$$

$$\begin{aligned} y_1 &= -d\sin\varphi - x_2\sin(\theta+\gamma+\varphi) \\ &+ y_2\cos(\theta+\gamma+\varphi), \end{aligned} \tag{22}$$

$$\begin{aligned} -y_1 - d_1\sin\varphi - x_2\sin(\theta+\gamma+\varphi) \\ + y_2\cos(\theta+\gamma+\varphi) = 0. \end{aligned} \tag{23}$$

Multiplying the first relation (20) by $\cos\varphi$, the second relation (20) by $\sin\varphi$ and summing the results, we obtain

$$\begin{aligned} x_1\cos^2\varphi + x_1\sin^2\varphi &= d\cos\varphi \\ &+ x_2\cos(\theta+\gamma)\cos\varphi \\ &+ y_2\sin(\theta+\lambda)\cos\varphi \\ &- x_2\sin(\theta+\gamma)\sin\varphi \\ &+ y_2\cos(\theta+\gamma)\sin\varphi, \end{aligned} \tag{24}$$

$$\begin{aligned} x_1 &= d\cos\varphi + x_2\cos(\theta+\gamma+\varphi) \\ &+ y_2\sin(\theta+\gamma+\varphi), \end{aligned} \tag{25}$$

$$\begin{aligned} -x_1 + d\cos\varphi + x_2\cos(\theta+\gamma+\varphi) \\ + y_2\sin(\theta+\gamma+\varphi) = 0. \end{aligned} \tag{26}$$

Calling now the relations (19) and replacing them in the expressions (23) and (26), one deduces the formulae

$$\begin{aligned} -y_1 - d\sin\varphi + (l_2 + R_3\sin\lambda) \\ \times\sin(\theta+\gamma+\varphi) \\ - R_3\cos\lambda\cos(\theta+\gamma+\varphi) = 0, \end{aligned} \tag{27}$$

$$\begin{aligned} -x_1 - d\cos\varphi - (l_2 + R_3\sin\lambda) \\ \times\cos(\theta+\gamma+\varphi) \\ - R_3\cos\lambda\sin(\theta+\gamma+\varphi) = 0, \end{aligned} \tag{28}$$

wherefrom

$$\begin{aligned} f_1(\varphi,\lambda) &= -x_1 + d\cos\varphi \\ &- l_2\cos(\theta+\gamma+\varphi) \\ &- R_3\sin(\theta+\gamma+\varphi+\lambda) = 0, \\ f_2(\varphi,\lambda) &= -y_1 - d\sin\varphi \\ &+ l_2\sin(\theta+\gamma+\varphi) \\ &- R_3\cos(\theta+\gamma+\varphi+\lambda) = 0. \end{aligned} \tag{29}$$

The profile of the cam is obtains as the envelope of the successive positions of the cam and, consequently, it is deduced from the equation

$$\begin{vmatrix} \frac{\partial f_1}{\partial\varphi} & \frac{\partial f_1}{\partial\lambda} \\ \frac{\partial f_2}{\partial\varphi} & \frac{\partial f_2}{\partial\lambda} \end{vmatrix} = 0, \tag{30}$$

where,

$$\begin{aligned} \frac{\partial f_1}{\partial\varphi} &= -d\sin\varphi + [l_2\sin(\theta+\gamma+\varphi) \\ &- R_3\cos(\theta+\gamma+\varphi+\lambda)]\left(1+\frac{d\theta}{d\varphi}\right), \end{aligned} \tag{31}$$

$$\frac{\partial f_1}{\partial\lambda} = -R_3\cos(\theta+\gamma+\varphi+\lambda) = 0, \tag{32}$$

$$\begin{aligned} \frac{\partial f_2}{\partial\varphi} &= -d\cos\varphi + [l_2\cos(\theta+\gamma+\varphi) \\ &+ R_3\sin(\theta+\gamma+\varphi+\lambda)]\left(1+\frac{d\theta}{d\varphi}\right), \end{aligned} \tag{33}$$

$$\frac{\partial f_2}{\partial\lambda} = R_3\sin(\theta+\gamma+\varphi+\lambda). \tag{34}$$

Relation (30) leads to the equalities:

$$
\begin{aligned}
&- dR_3 \sin\varphi \sin(\theta+\gamma+\varphi+\lambda) \\
&+ l_2 R_3 \sin(\theta+\gamma+\varphi)\times \\
&\sin(\theta+\gamma+\varphi+\lambda)\left(1+\frac{d\theta}{d\varphi}\right) \\
&-\left(1+\frac{d\theta}{d\varphi}\right)R_3^2\cos(\theta+\gamma+\varphi+\lambda) \\
&\times\sin(\theta+\gamma+\varphi+\lambda) - dR_3\cos\varphi \\
&\times\cos(\theta+\gamma+\varphi+\lambda)+\left(1+\frac{d\theta}{d\varphi}\right) \\
&\times\left[l_2 R_3\cos(\theta+\gamma+\varphi)\right. \\
&\times\cos(\theta+\gamma+\varphi+\lambda)+R_3^2 \\
&\left.\times\sin(\theta+\gamma+\varphi+\lambda)\cos(\theta+\gamma+\varphi+\lambda)\right], \\
&- dR_3\cos(\theta+\gamma+\varphi) \\
&+ l_2 R_3\cos\lambda\left(1+\frac{d\theta}{d\varphi}\right)=0,
\end{aligned}
\tag{35}
$$

$$
\begin{aligned}
&- dR_3\cos(\theta+\gamma)\cos\lambda \\
&+ dR_3\sin(\theta+\gamma)\sin\lambda \\
&+ l_2 R_3\cos\lambda\left(1+\frac{d\theta}{d\varphi}\right)=0,
\end{aligned}
\tag{36}
$$

$$
\begin{aligned}
&d\sin(\theta+\gamma)\sin\lambda = \\
&\left[d\cos(\theta+\gamma)-l_2\left(1+\frac{d\theta}{d\varphi}\right)\right]\cos\lambda,
\end{aligned}
\tag{37}
$$

$$
\begin{aligned}
&d\cos(\theta+\gamma)\sin\lambda = \\
&\left[d\sin(\theta+\gamma)+l_2\left(1+\frac{d\theta}{d\varphi}\right)\right]\cos\lambda,
\end{aligned}
\tag{38}
$$

wherefrom

$$
\operatorname{tg}\lambda=\frac{d\cos(\theta+\gamma)-l_2\left(1+\frac{d\theta}{d\varphi}\right)}{d\sin(\theta+\gamma)}.
\tag{39}
$$

From the last relation can calculate the parameter λ, while the parametric equations of the cam's profile are deduced from the (29).

The derivatives $\frac{d\theta}{d\varphi}$ and $\frac{d^2\theta}{d\varphi^2}$ which give the reduced angular velocity and acceleration are given by

$$
\left.\frac{d\theta}{d\varphi}\right|_{\varphi=\varphi_i}=\frac{\theta_{i+1}-\theta_{i-1}}{2\Delta\varphi},
\tag{40}
$$

$$
\left.\frac{d^2\theta}{d\varphi^2}\right|_{\varphi=\varphi_i}=\frac{\theta_{i+1}-2\theta_i+\theta_{i-1}}{(\Delta\varphi)^2},
\tag{41}
$$

where $\Delta\varphi$ is 1° or $\frac{\pi}{180}$ rad.

4. NUMERICAL EXAMPLE

As numerical example we consider the case defined by $l_1=0.01612\,\text{m}$, $R_1=0.025\,\text{m}$, $R_2=0.010\,\text{m}$, $\beta_0=15^\circ$, $s_{\max}=0.00935\,\text{m}$, $R_0=0.018\,\text{m}$, the opening angles of the valve $\varphi_1=92^\circ$, $\varphi_2=161^\circ$ (the angle at which the valve is completely open), the closing angles of the valve $\varphi_3=180^\circ$, $\varphi_4=244^\circ$ (the angle at which the valve is completely closed), the angular step $\Delta\varphi=1^\circ$, $d=0.042\,\text{m}$, $l_2=0.06\,\text{m}$, $R_3=0.01867\,\text{m}$ and two laws of displacement of the valve

$$
s_1(\varphi)=\begin{cases}
0 \text{ for } \varphi\in[0,\varphi_1), \\
s_{\max}\sin^2\left(\dfrac{90(\varphi-\varphi_1)}{\varphi_2-\varphi_1}\right) \\
\text{for } \varphi\in[\varphi_1,\varphi_2], \\
s_{\max} \text{ for } \varphi(\varphi_2,\varphi_3), \\
s_{\max}\sin^2\left(\dfrac{90(\varphi+\varphi_4-2\varphi_3)}{\varphi_4-\varphi_3}\right) \\
\text{for } \varphi\in[\varphi_3,\varphi_4], \\
0 \text{ for } \varphi\in(\varphi_4,360],
\end{cases}
\tag{42}
$$

$$
s_2(\varphi)=\begin{cases}
0 \text{ for } \varphi\in[0,\varphi_1), \\
s_{\max}\dfrac{(\varphi-\varphi_1)^2(\varphi-2\varphi_2+\varphi_1)^2}{(\varphi_2-\varphi_1)^4} \\
\text{for } \varphi\in[\varphi_1,\varphi_2], \\
s_{\max} \text{ for } \varphi(\varphi_2,\varphi_3), \\
s_{\max}\dfrac{(\varphi-\varphi_4)^2(\varphi-2\varphi_3+\varphi_4)^2}{(\varphi_3-\varphi_4)^2} \\
\text{for } \varphi\in[\varphi_3,\varphi_4], \\
0 \text{ for } \varphi\in(\varphi_4,360].
\end{cases}
\tag{43}
$$

The angle β of rotation of the lever is determined from the equation (14).

The corresponding cams are drawn in Figure 4 and Figure 5. The blue color corresponds to the cams obtained by synthesis, while the red color corresponds to the convex cam obtained by applying the Jarvis march to the original cams. The reduced angular velocities and accelerations are drawn in Figures 6 – 9.

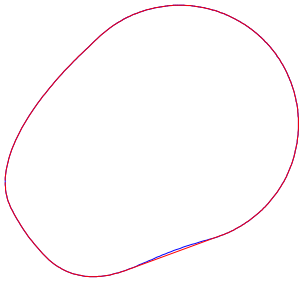

Fig. 4. The cam obtained using the first law of displacement for the valve

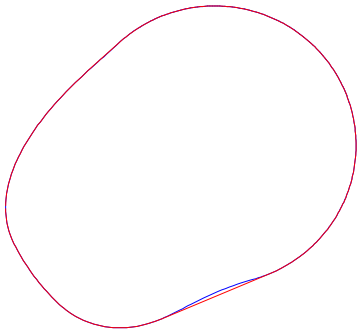

Fig. 5. The cam obtained using the second law of displacement for the valve

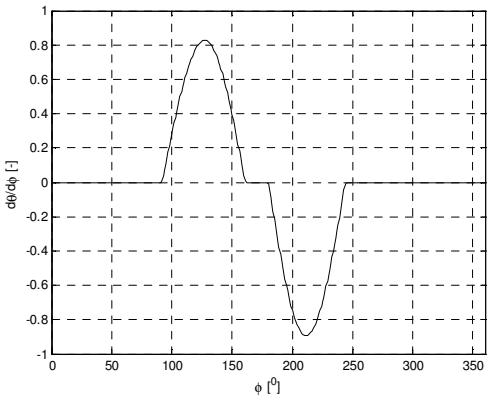

Fig. 6. The reduced angular velocity using the first law of displacement for the valve

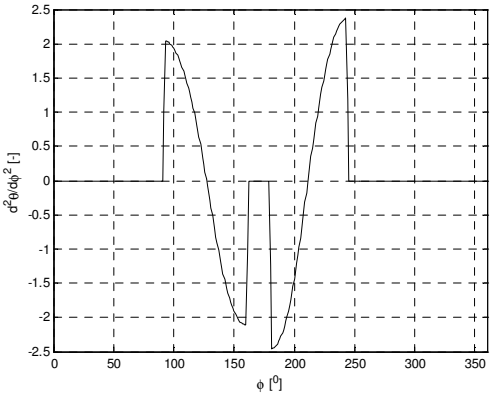

Fig. 7. The reduced angular acceleration using the first law of displacement for the valve

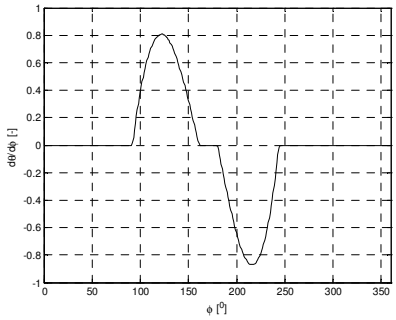

Fig. 8. The reduced angular velocity using the second law of displacement for the valve

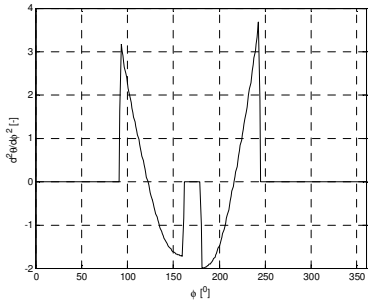

Fig. 9. The reduced angular acceleration using the second law of displacement for the valve

5. THE CASE OF THE PLANAR HEAD OF VALVE

The working schema is presented in Fig. 10. One obtains the geometric relations

$$h = l_1 \sin\beta_0 + R_2\,, \tag{44}$$

$$h + s = l_1 \sin\beta + R_2\,, \tag{45}$$

wherefrom it results by subtracting

$$s = l_1(\sin\beta - \sin\beta_0)\,; \tag{46}$$

hence

$$\sin\beta = \frac{s + l_1 \sin\beta_0}{l_1}\,, \tag{47}$$

$$\beta = \arcsin\left(\frac{s + l_1 \sin\beta_0}{l_1}\right). \tag{48}$$

We may also write

$$\theta = \beta - \beta_0 = \arcsin\left(\frac{s + l_1 \sin\beta_0}{l_1}\right) - \beta_0 \tag{49}$$

and from here one deduces the formula

$$\frac{d\theta}{d\varphi} = \frac{d\theta}{ds}\frac{ds}{d\varphi} = \frac{1}{\sqrt{1 - \left(\frac{s + l_1 \sin\beta_0}{l_1}\right)^2}}\frac{ds}{d\varphi}\,. \tag{50}$$

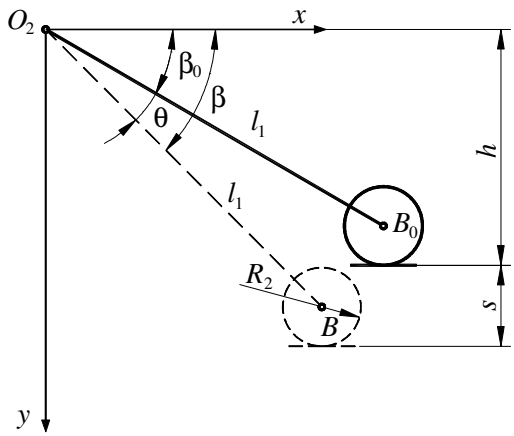

Fig. 10. The case of planar head of valve

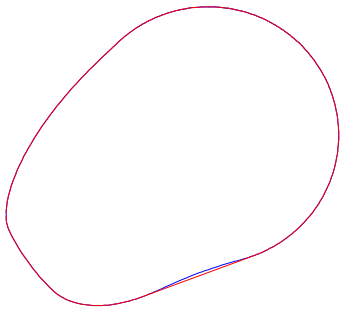

Fig. 11. The cam obtained using the first law of displacement for the valve

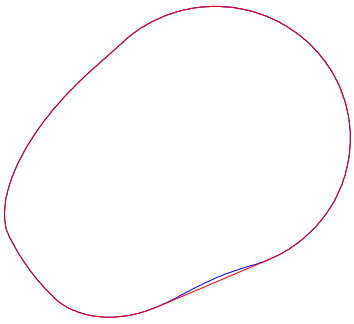

Fig. 12. The cam obtained using the second law of displacement for the valve

6. NUMERICAL EXAMPLE

We consider the same numerical example as in paragraph 4, the difference being that now the head of the valve is a planar one.

The obtained diagrams are drawn in Figs. 11 – 16. The code of the colors is the same.

7. CONCLUSION

The two laws of displacement for the valve lead to similar values for the reduced angular velocities and accelerations.

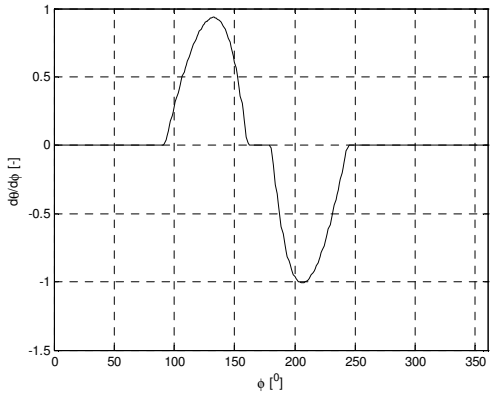

Fig. 13. The reduced angular velocity using the first law of displacement for the valve

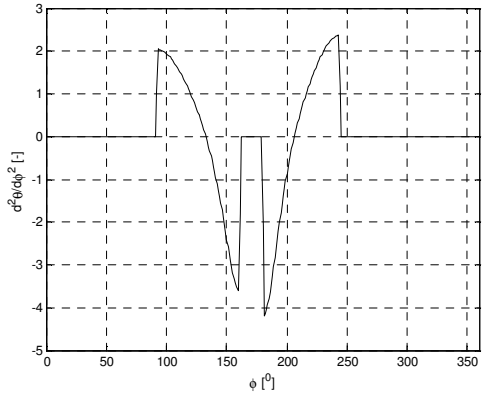

Fig. 14. The reduced angular acceleration using the first law of displacement for the valve

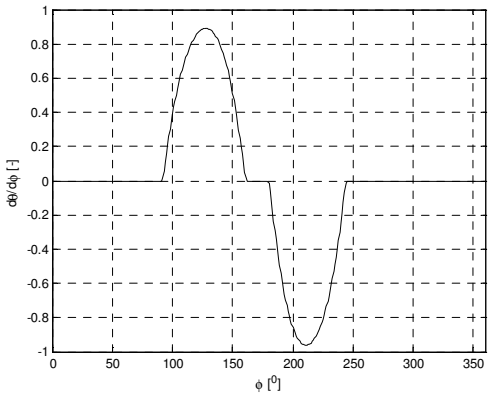

Fig. 15. The reduced angular velocity using the second law of displacement for the valve

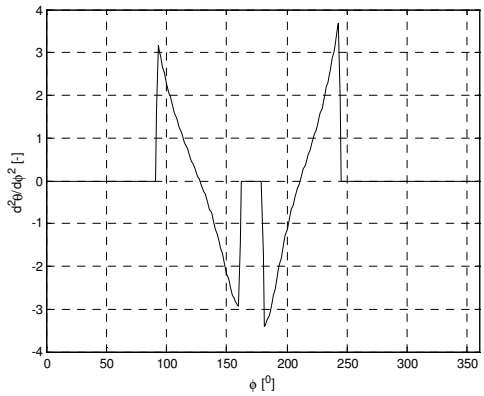

Fig. 16. The reduced angular acceleration using the second law of displacement for the valve

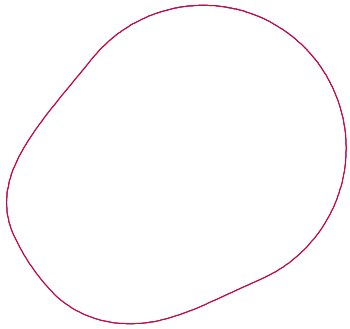

Fig. 17. The cam obtained using the first law of displacement for the valve, spherical head of valve, and the new value for the radius of the base circle

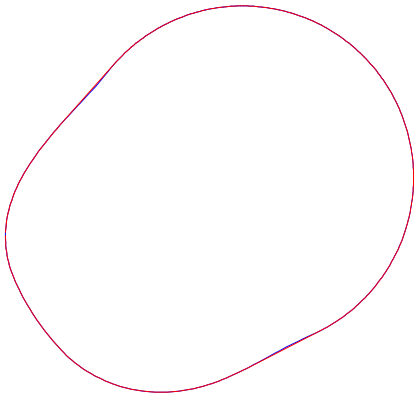

Fig. 18. The cam obtained using the second law of displacement for the valve, spherical head of valve, and the new value for the radius of the base circle

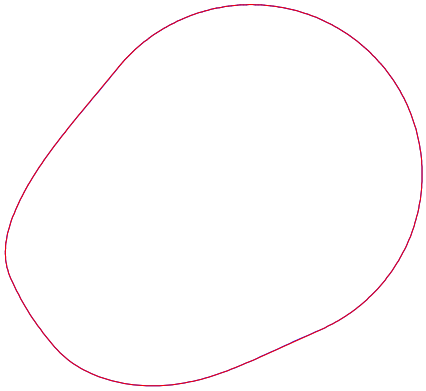

Fig. 19. The cam obtained using the first law of displacement for the valve, planar head of valve, and the new value for the radius of the base circle

The cam for the Miller – Atkinson cycle is, in general, a not a convex one.

Modifying the radius of the base circle of cam to the new value $R_0 = 0.025\,\mathrm{m}$, we obtain a new diagrams captured in Figs. 17 – 28. Again, we used the same code of colors.

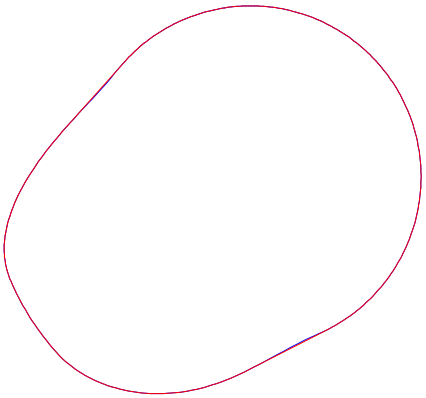

Fig. 20. The cam obtained using the second law of displacement for the valve, planar head of valve, and the new value for the radius of the base circle

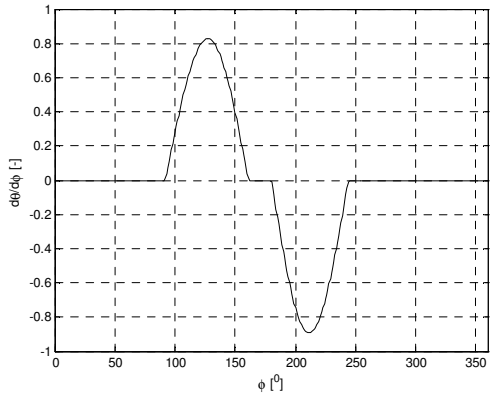

Fig. 21. The reduced angular velocity using the first law of displacement for the valve, spherical head of valve, and the new value for the radius of the base circle

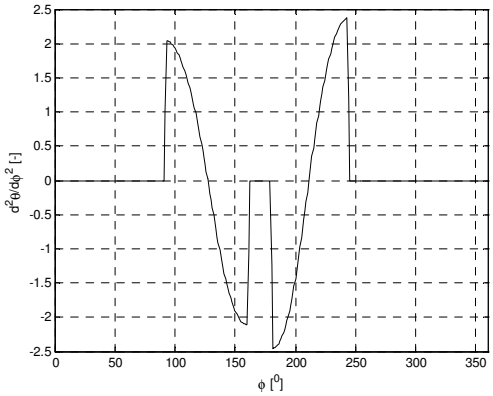

Fig. 22. The reduced angular acceleration using the first law of displacement for the valve, spherical head of valve, and the new value for the radius of the base circle

To be out to obtain convex cams, we had to apply the Jarvis march. The difference between the two cams is a small one.

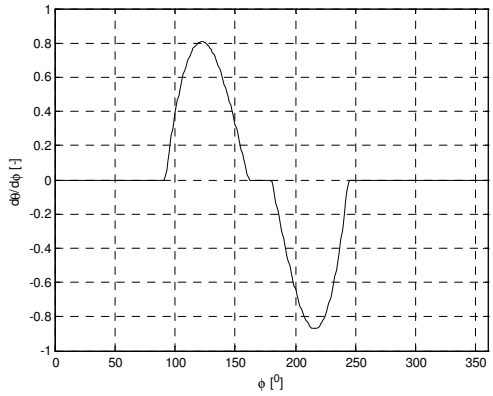

Fig. 23. The reduced angular velocity using the second law of displacement for the valve, spherical head of valve, and the new value for the radius of the base circle

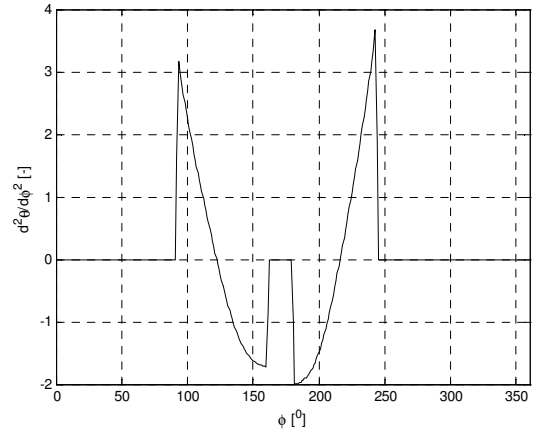

Fig. 24. The reduced angular acceleration using the second law of displacement for the valve, spherical head of valve, and the new value for the radius of the base circle

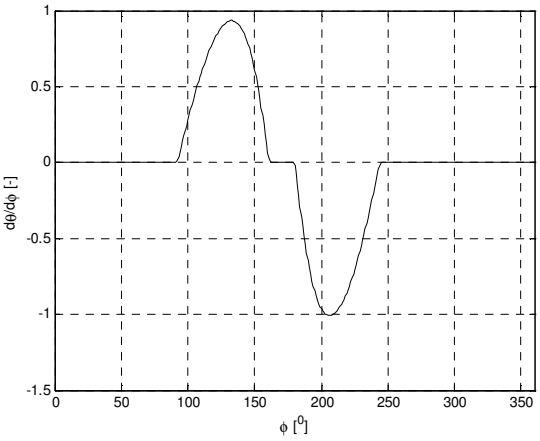

Fig. 25. The reduced angular velocity using the first law of displacement for the valve, planar head of valve, and the new value for the radius of the base circle

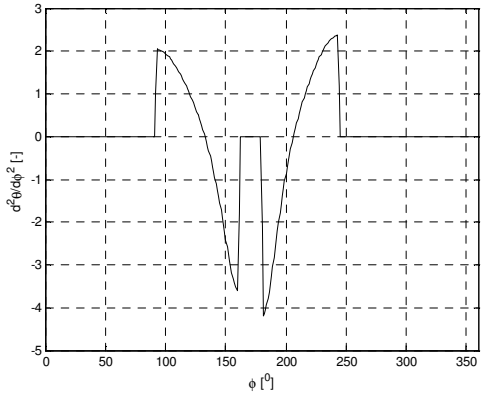

Fig. 26. The reduced angular acceleration using the first law of displacement for the valve, planar head of valve, and the new value for the radius of the base circle

The variation of the parameter λ is presented in the Figures 29 – 32.

The shape of the curves of reduced angular velocities and accelerations are almost the same for all considered cases.

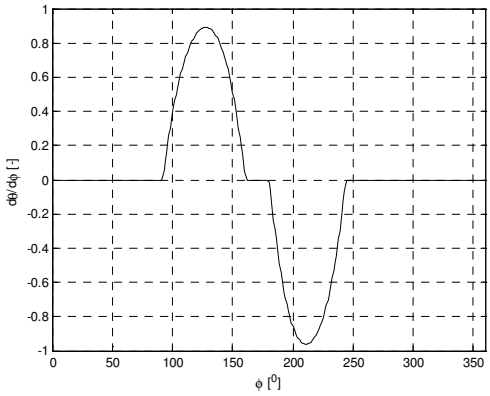

Fig. 27. The reduced angular velocity using the second law of displacement for the valve, planar head of valve, and the new value for the radius of the base circle

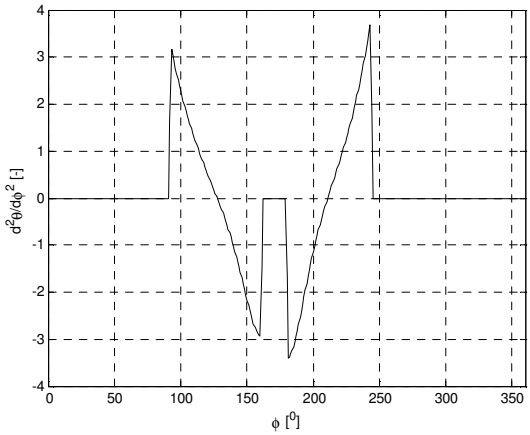

Fig. 28. The reduced angular acceleration using the second law of displacement for the valve, planar head of valve, and the new value for the radius of the base circle

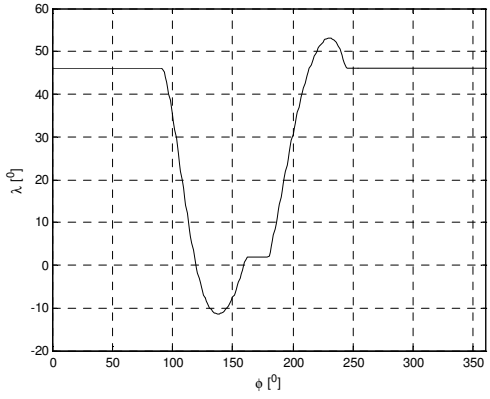

Fig. 29. The variation of the parameter λ using the first law of displacement for the valve, spherical head of valve, and the original value for the radius of the base circle

The spherical head of valve has the tendency to lead to not convex cams. The tendency is

kept for the planar head, but the difference between the cams is smaller.

One may observe that there exist great difference between the extreme values of the parameter λ for each case, but the shape of the curve $\lambda = \lambda(\theta)$ remains unchanged, no matter the situation considered in our study.

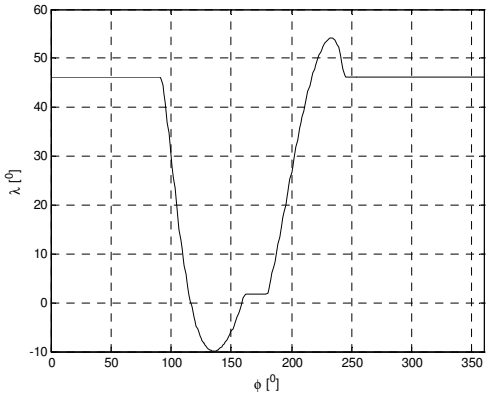

Fig. 30. The variation of the parameter λ using the second law of displacement for the valve, spherical head of valve, and the original value for the radius of the base circle

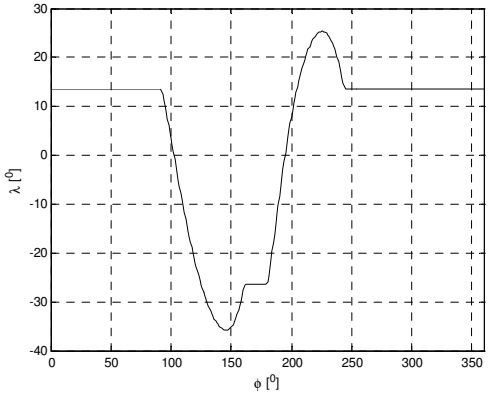

Fig. 31. The variation of the parameter λ using the first law of displacement for the valve, planar head of valve, and the new value for the radius of the base circle

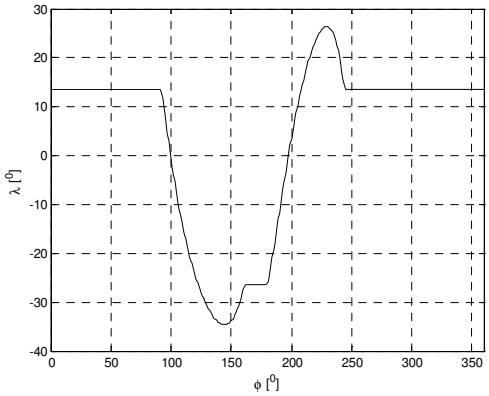

Fig. 32. The variation of the parameter λ using the second law of displacement for the valve, planar head of valve, and the new value for the radius of the base circle

The influence of other different parameters (e.g. lengths of the elements etc.) on the cam's profile and on different kinematic and dynamic parameters will be studied in future papers.

REFERENCES

[1] Gonca, G., Sahin, B., Parlak, A., Ust, Y., Ayhan, V., Cesur, I., Boru, B., *Theoretical and experimental investigation of the Miller cycle diesel engine in terms of performance and emission parameters*, Applied Energy 138 (2015) 11–20.

[2] Martins, M., E., S., Lanzanova, T., D., M., *Full-load Miller cycle with ethanol and EGR: Potential benefits and challenges*, Applied Thermal Engineering 90 (2015) 274–285.

[3] Ebrahimi, R., *Effects of mean piston speed, equivalence ratio and cylinder wall temperature on performance of an Atkinson engine*, Mathematical and Computer Modelling 53 (2011) 1289–1297.

[4] Zammit, J., P., McGhee, M., J., Shayler, P., J., Lawa, T., Pegg, I., *The effects of early inlet valve closing and cylinder disablement on fuel economy and emissions of a direct injection diesel engine*, Energy 79 (2015) 100-110.

[5] Murata, Y., Kusaka, J., Odaka, M., Daisho, Y., Kawano, D., Suzuki, H., Ishii, H., Goto, Y., *Achievement of medium engine speed and load premixed diesel combustion with variable valve timing*, SAE paper 2006-01-0203, 2006.

[6] De Ojeda ,W., *Effect of variable valve timing on diesel combustion characteristics*. SAE paper 2010-01-1124, 2010.

[7] Kéromnčs, A., Delaporte, B., Schmitz, G., Le Moyne, L., *Development and validation of a 5 stroke engine for range extenders application*, Energy Conversion and Management 82 (2014) 259–267.

[8] Zhu, S., Deng, K., Liu, S., Qu, S., *Comparative analysis and evaluation of turbocharged Dual and Miller cycles under different operating conditions*, Energy 93 (2015) 75-87.

[9] Mihalcea, S., Stănescu, N.-D., Popa, D., *Synthesis and kinematic and dynamic*

analysis of a variable valve lift mechanism with general contact curve, Proceedings of the International Institution of Mechanical Engineers, Part K, Journal of Multi-body Systems, vol. 229(1), Pages 65–83, 2015, DOI: 10.1177/1464419314546921.

[10] Stănescu, N.-D., Popa, D., *The Vibrations of the Engine with Neo-Hookean Suspension*, Acoustics & Vibration of Mechanical Structures, Applied Mechanics and Materials, vol. 430, 53-59, 2013.

[11] Stănescu, N.–D., Popa, D., *Stability of the equilibrium positions of an engine with nonlinear quadratic springs*, CEJE, 4(2), 2014, pp.170-177, DOI: 10.2478/s13531-013-0138-1.

[12] Stănescu, N.–D., Dragomir, I., Pandrea, N., Clenci, A., Popa, D., *Geometric Constraints at the Distribution Mechanism with Spherical Contact between the Lever and the Head of the Valve*, Proceedings of International Automotive Congress, CONAT 2016, ISBN 2069-0401, 43-51, 2016.

[13] Dragomir, I., Mănescu, B., Stănescu, N.-D., *The Analysis of a Distribution Mechanism for the Miller-Atkinson Cycle*, AVMS 2017, Timișoara, 2017.

SINTEZA CAMEI ȘI DETERMINAREA VITEZEI ȘI ACCELERAȚIEI REDUSE ALE CULBUTORULUI UNUI MECHANISM DE DISTRIBUȚIE PENTRU CICLUL MILLER – ATKINSON

Abstract: *În această lucrare se consideră un mechanism de distribuție folosit pentru ciclul Miller – Atkinson al unui motor. Sinteza camei este realizată cu ajutorul metodelor numerice și folosind considerații geometrice. Au fost considerate două legi de mișcare pentru deplasarea supapei. În fiecare caz s-au calculat viteza și accelerația unghiulare reduse. Capul supapei a fost considerat sferic sau plan. S-a studiat și influența diferiților parametri asupra vitezei și accelerației unghiulare reduse a culbutorului.*

Ionuț DRAGOMIR, drd. ing., AKKA Romserv, București, Universitatea din Pitești, Departamentul de Fabricație și Management Industrial, e-mail: ionut.dragomir1988@gmail.com, Office Phone: 0348453155, Home Phone 0740950087

Bogdan MĂNESCU, drd. ing., AKKA Romserv, București, Universitatea din Pitești, Departamentul de Fabricație și Management Industrial, e-mail: bogdan.manescu04@gmail.com, Office Phone: 0348453155,Home Phone 0766661647

Nicolae-Doru Stănescu, prof. univ. dr. ing. habil. dr. mat., Universitatea din Pitești, Departamentul de Fabricație și Management Industrial, e-mail: doru.stanescu@upit.ro, s_doru@yahoo.com, Office Phone: 0348453155, Home Address: Pitești, str. Matei Basarab, nr. 22, cod 110227, Home Phone 0745050055.

Nicolae PANDREA, prof. univ. emerit dr. ing., membru al Academiei de Științe Tehnice din România, vicepreședinte Secția de Mecanică, Universitatea din Pitești, Departamentul de Fabricație și Management Industrial, e-mail: nicolae_pandrea37@yahoo.com, Office Phone: 0348453155, Home Address: Bascov, str. Rotărești Foraj, nr. 71B, Home Phone 0723395567.